Corrosion Science 52 (2010) 3891–3895

Contents lists available at ScienceDirect

Corrosion Science

journal homepage: www.elsevier.com/locate/corsci

A corrosion study of nanocrystalline copper thin films

Edilson M. Pinto [a], A. Sofia Ramos [b], M. Teresa Vieira [b], Christopher M.A. Brett [a,*]

[a] CEMUC®, Departamento de Química, Faculdade de Ciências e Tecnologia, Universidade de Coimbra, 3004-535 Coimbra, Portugal
[b] CEMUC®, Departamento de Engenharia Mecânica, Faculdade de Ciências e Tecnologia, Universidade de Coimbra, 3030-788 Coimbra, Portugal

ARTICLE INFO

Article history:
Received 5 June 2010
Accepted 6 August 2010
Available online 10 August 2010

Keywords:
A. Copper
A. Sputtered films
B. EIS
B. Polarization
B. SEM

ABSTRACT

Thin nanocrystalline, compact films, based on the copper–nitrogen system, up to 2.5 μm thickness and 3.5% nitrogen, were deposited by magnetron sputtering at different partial pressure ratios of N_2 and Ar, without formation of Cu_xN compounds, the nitrogen concentration influencing grain size (down to 30 nm) and film homogeneity. Electrochemical corrosion properties were investigated using polarization curves and electrochemical impedance spectroscopy in 0.5 M NaCl aqueous solution, and compared with pure bulk copper; morphology was examined by scanning electron microscopy. Significant variations in corrosion currents between samples were attributed to grain size and structural defects on the grain boundaries.

1. Introduction

It is well known that copper is one the most important industrial materials with a wide variety of applications due to its excellent electrical, thermal and mechanical properties and corrosion resistance. New industrial challenges require the production of improved high strength/ductile copper, reflected by the research for over two decades on nanocrystalline materials with a strong focus on copper. However, for nanocrystalline copper to be widely used, it is necessary to study in detail the effects of nanocrystallinity on its other properties, such as corrosion resistance [1].

Sputtering is one of the most efficient techniques to produce nanocrystalline thin film materials, and is often used to study "new" properties of nanocrystalline bulk materials. Control of the film deposition parameters is one of the advantages of the sputtering technique, another being that it can dope materials with elements beyond their equilibrium solubility, to control structures and morphologies [2]. Copper is one of the few metallic elements with high adatom mobility whilst exhibiting low susceptibility to nanocrystallinity [2,3]. Fabrication of nanocrystalline copper thin films by sputtering is carried out with the substrate assisted by a cold trap, or more recently using a controlled atmosphere with different partial pressures of nitrogen [2].

In recent work [2], different thin films based on the Cu–N system were deposited by reactive magnetron sputtering with a compact cauliflower morphology, employing partial pressure ratios of nitrogen and argon, $P_{N_2} : P_{Ar}$ less than 1:2. Under these conditions it was possible to incorporate nitrogen into copper thin films without the formation of CuN compounds. Although a heterogeneous nitrogen distribution through the films was observed, it was found that the grain size distribution was homogeneous, even at the lowest nitrogen content, as well as a significant decrease in grain size down to 30 nm compared to sputtering in the absence of nitrogen. Besides the unexpected and remarkable impact of this result on the mechanical properties of copper films, a question to answer is how the nanocrystallinity of the metal influences the electrochemical properties of the films, especially the corrosion resistance.

An important quality of this metal and its alloys is its resistance to corrosion attributed to the formation of a protective film of cuprous oxide (Cu_2O) [4,5]. However, in the presence of oxygen, chlorides, sulphates or nitrate ions, the metal is susceptible to localized types of corrosion such as pitting corrosion, which is very dangerous for thin film structures [6], and two possible mechanisms for the observed increase of corrosion rate have been proposed [7–11]. These are the dissolution-precipitation mechanism and the erosion mechanism. Electrochemical, accelerated corrosion techniques have been presented as an alternative tool for the investigation of the copper corrosion mechanism; the advantages are decreasing the experimental time and improving the data reproducibility.

Traditional dc polarization methods as well as ac techniques such as electrochemical impedance spectroscopy (EIS) are useful in characterizing the corrosion behaviour. One of the principal advantages of EIS is that it can be performed in solutions of low conductivity, which is a problem that may affect dc electrochemical measurements [12]. Also, EIS is a non-destructive technique (only a small perturbation signal is applied during the measurements), so that EIS measurements at the open circuit potential can be repeated several times without altering the surface of the

* Corresponding author. Tel./fax: +351 239 835295.
E-mail address: brett@ci.uc.pt (C.M.A. Brett).

0010-938X/$ - see front matter © 2010 Elsevier Ltd. All rights reserved.
doi:10.1016/j.corsci.2010.08.001

metal being examined [13]. A number of papers have been devoted to the study of the corrosion and corrosion inhibition of copper and its alloys with elucidation of the mechanisms, especially in NaCl environments simulating seawater [14–19].

The present work was undertaken to investigate the corrosion behaviour of different nanograined copper thin films in chloride media, prepared by magnetron sputtering, using linear sweep voltammetry (Tafel plots) and EIS. Additionally, the samples were examined with scanning electron microscopy (SEM) in order to give important information concerning the morphology and the surface characteristics before and after the occurrence of corrosion.

2. Materials and methods

2.1. Copper deposition

Cu and Cu–N thin films were deposited by dc magnetron sputtering on square stainless steel substrates of area 1 cm^2. In the case of the Cu–N thin films, the copper target was sputtered in reactive mode using three different nitrogen/argon partial pressure ratios (P_{N_2} : P_{Ar}) 1:60 (1 of nitrogen to 60 parts of argon), 1:30 and 1:2. A total deposition pressure of 0.3 Pa and a constant power density of the pure copper target of 3.33 W mm^{-2} were used. In order to avoid grain growth during deposition, the substrate temperature was maintained at a temperature lower than 373 K by promoting heat flow through the substrate holder to the exterior of the sample. The sputtering chamber was evacuated to 2×10^{-4} Pa before admitting pure argon and nitrogen gases.

Thin copper films produced were as follows: Cu(N0.0) – 2.5 μm thick without nitrogen, Cu(N1.5) – 2.5 μm with 1.5% nitrogen, and Cu(N3.5) – 1.5 μm thick with 3.5% nitrogen. The Cu–N films are all nanocrystalline, with grain size decreasing down to 30 nm with 3.5 at.% of nitrogen [2].

2.2. Reagents and electrolyte solutions

Millipore Milli-Q nanopure water (resistivity $\geqslant$18 MΩ cm) and analytical reagents were used for the preparation of all solutions. Experiments were performed at room temperature (25 ± 1 °C), and 0.5 M NaCl aqueous solution, in the presence of dissolved O_2, was used as electrolyte.

Electrodes were made by attaching a copper wire to the rear surface of the stainless steel substrates with silver conductive paint covered by epoxy resin, insulating the rest of the stainless steel surface and edges with epoxy resin, leaving only the deposited copper thin films exposed. For comparison purposes, electrodes of pure bulk copper (99.99%, Johnson–Matthey, area 0.20 cm^2) were also made; these were polished with alumina down to 0.3 μm particle size before use.

A three-electrode electrochemical cell of volume 10 cm^3 was used, containing the copper electrode as working electrode, a platinum foil counter electrode and a saturated calomel electrode (SCE) as reference.

Electrochemical measurements were performed using a computer-controlled μ-Autolab Type II potentiostat–galvanostat running with GPES (General Purpose Electrochemical System) for Windows Version 4.9 software (Metrohm Autolab, Utrecht, Netherlands).

The electrochemical impedance measurements were carried out on a PC-controlled Solartron 1250 Frequency Response Analyser, coupled to a Solartron 1286 Electrochemical Interface using ZPlot 2.4 software (Solartron Analytical, UK). A rms perturbation of 10 mV was applied over the frequency range 65 kHz–0.01 Hz, with 10 frequency values per decade.

A Philips XL-30 scanning electron microscope was used for surface morphology characterization. All images were captured using 15 keV.

3. Results and discussion

3.1. Polarization curves

In order to investigate the electrochemical properties of the copper thin films, electrochemical measurements using linear sweep voltammetry were carried out in 0.5 M NaCl aqueous solution in the presence of dissolved O_2 in the applied potential range from −500 mV vs. to +500 mV vs. SCE, at 5 mV s^{-1} scan rate. Fig. 1 shows the corresponding Tafel plots for all experiments, both bulk copper electrode and Cu(N1.5) had lower anodic and cathodic currents, with a positive potential shift of 30 mV of E_{cor} for the thin films.

The anodic and cathodic currents are generally lower at the bulk electrode. Except for the Cu(N3.5) electrode, evidence of barrier oxide film formation is observed, with dissolution at ∼+0.2 V vs. SCE.

The Cu(N0.0) electrodes showed higher currents than the bulk electrodes at all potentials, but the currents at Cu(N3.5) and Cu(N1.5) are lower than the values obtained for Cu(N0.0). The determination of I_{cor} is strongly influenced by the shape of the curve and the applied experimental methodology [20,21]. The values of E_{cor} and I_{cor}, estimated from extrapolation of the linear parts of the Tafel plots, are presented in Table 1. As seen, all the samples have similar corrosion potential values, with a variation of ±15 mV vs SCE. However, the I_{cor} values vary significantly, ranging from 0.12 μA cm^{-2} for Cu(N1.5) films, to 6.99 μA cm^{-2} for the Cu(N3.5) films.

The experiments using all three types of copper film electrodes (Cu(N0.0), Cu(N3.5) and Cu(N1.5)) were very reproducible, a similar I_{cor} being obtained from five electrodes of each type, the same being true of the Tafel slopes, as shown in Table 1. Table 1 also shows the potentials at open circuit recorded after 15 min immersion, when the values have reached a much slower variation with time, are also shown and are more positive by approximately 100 mV than the corrosion potentials, this difference demonstrating that a stationary state has not yet been reached. Long term measurements of steady-state OCP were not possible on some of the samples since, in those cases, the films began to degrade.

The results obtained by potentiodynamic measurements show that the nanocrystallinity of the copper films influences their elec-

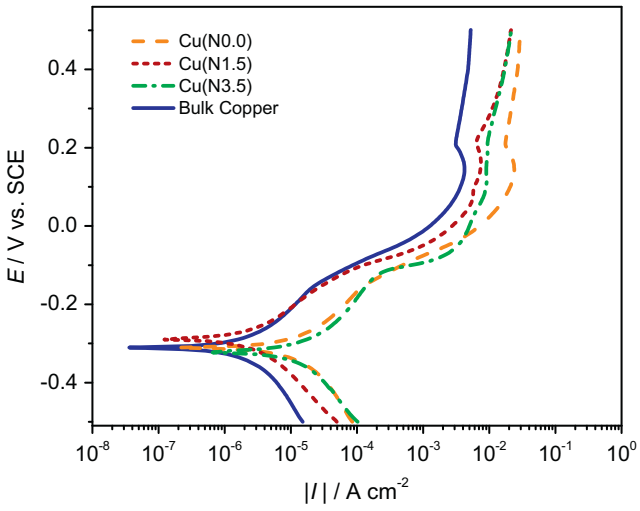

Fig. 1. Tafel plots for all types of electrode in 0.5 M NaCl, scan rate 5 mV s^{-1}.

Table 1
Corrosion parameters obtained from Tafel Plots (E_{cor}, I_{cor} and Tafel slopes β_a and β_c) and OCP after 15 min immersion, for all types of electrode in 0.5 M NaCl in the presence of dissolved O_2; data for five electrodes.

	Sample type			
	Cu (N0.0)	Cu (N1.5)	Cu (N3.5)	Bulk Cu
E_{cor}/mV vs. SCE	−283 ± 16	−323 ± 10	−313 ± 2	−313 ± 7
I_{cor}/μA cm^{-2}	2.62 ± 0.92	0.12 ± 0.08	6.99 ± 1.03	1.87 ± 0.89
β_a/V dec^{-1}	0.72 ± 0.03	0.12 ± 0.04	0.10 ± 0.01	0.09 ± 0.005
β_c/V dec^{-1}	0.17 ± 0.01	0.19 ± 0.02	0.18 ± 0.01	0.20 ± 0.01
OCP/mV vs. SCE	−195 ± 3	−215 ± 3	−203 ± 8	−190 ± 5

Table 2
Chemical elements detected by EDX and the atomic percentage on the electrode surface after corrosion. Nitrogen, if present, was below the detection level.

Cu (N0.0)		Cu (N1.5)		Cu (N3.5)	
Element	at.%	Element	at.%	Element	at.%
O	63	O	65	O	54
Cl	12	Cl	11	Cl	6
Cu	25	Cu	24	Cu	40

trochemical behaviour. The Cu(N3.5) electrode is formed from the smallest grains of copper, so that it is expected that this electrode will have the higher corrosion current. Experiments with linear sweep voltammetry undertaken at other electrodes prepared with the same films reproduce the results described very closely.

3.2. EIS

Electrochemical impedance spectroscopy (EIS) experiments were carried out in 0.5 M NaCl, after a stabilization time of 15 min, at potentials equal to E_{cor} determined from Tafel analysis as well as at the OCP. Spectra were recorded at other potentials, in the range between −0.8 and +0.8 V vs SCE, but – partly due to the time needed to record a full impedance spectrum – the differences between the behaviour of the different films were less evident and so are not shown here.

The equivalent circuit proposed to fit the EIS results, similar to that proposed in other copper thin film electrode studies, e.g. [18], and is shown in Fig. 2. It consists of the cell resistance, R_Ω, with a value of 3 ± 0.5 Ω cm^2, in series with a parallel combination of a constant phase element, CPE$_1$ = $\{(Ci\omega)^n\}^{-1}$, representing the interfacial charge separation, modelled as a non-ideal capacitor, and a polarization resistance, R_1. Values of the n exponent were ~0.76 for all spectra.

Fig. 3 shows spectra recorded at E_{cor}. In all cases depressed semicircles were observed with a similar profile, differing only in the resistance and capacitance values. Table 3 presents the results obtained by fitting. It is seen that the smallest charge transfer resistance is obtained at the Cu(N3.5) electrode with a charge transfer resistance of 1.66 kΩ cm^2, while the bulk copper film electrode has the highest value of 4.44 kΩ cm^2. High capacitance values were

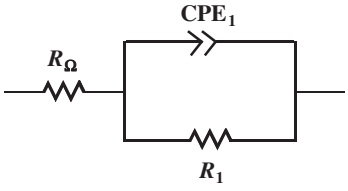

Fig. 2. Equivalent circuit proposed to fit the EIS results which represents the cell resistance, R_Ω, in series with a constant phase element, CPE1 representing the interfacial charge separation, in parallel with a polarization resistance, R_1.

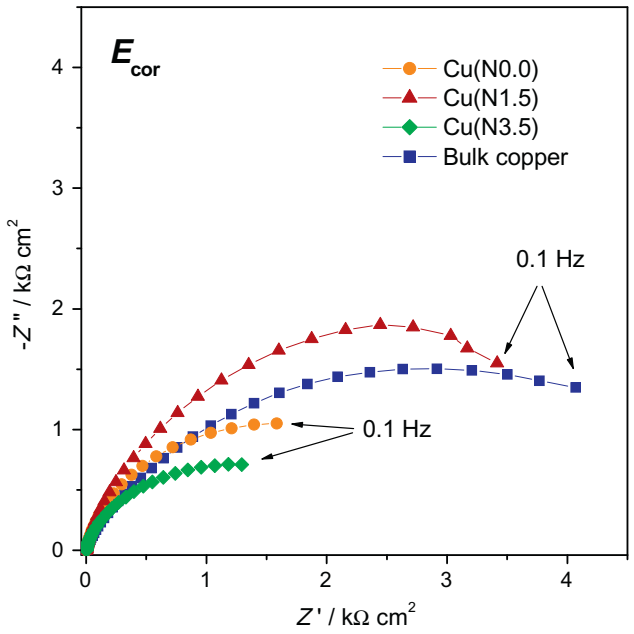

Fig. 3. Complex plane impedance plots in 0.5 M NaCl of: (●) Cu(N0.0), (▲) Cu(N1.5), (◆) Cu(N3.5), (■) bulk copper electrodes at applied potential equal to E_{cor} (see Table 1).

Table 3
Resistance and capacitance values obtained by equivalent circuit (Fig. 2) modelling of the impedance spectra (Fig. 3). The applied potentials corresponding to E_{cor}, are shown in Table 1.

	E_{cor}			
	Cu(N0.0)	Cu(N1.5)	Cu(N3.5)	Bulk Cu
R_1/kΩ cm^2	2.48	4.39	1.66	4.44
C_1/μF cm^{-2} s^{n-1}	233	72	204	60

Table 4
Resistance and capacitance values obtained by equivalent circuit (Fig. 2) modelling of the impedance spectra (Fig. 4). The values of OCP applied to each sample are shown in Table 1.

	OCP			
	Cu(0.0)	Cu(N1.5)	Cu(N3.5)	Bulk Cu
R_1/kΩ cm^2	3.87	0.52	0.50	1.96
C_1/μF cm^{-2} s^{n-1}	259	111	187	60

obtained for Cu(N0.0) and for Cu(N3.5) of 233 μF cm^{-2} s^{n-1} and 204 μF cm^{-2} s^{n-1}, respectively, much larger than the value of 72 μF cm^{-2} s^{n-1} for Cu(N1.5) and 60 μF cm^{-2} s^{n-1} for the bulk copper electrode.

Fig. 4 shows spectra recorded at all electrodes at applied potentials corresponding to the value of the OCP after 15 min immersion. At this potential the Cu(N1.5) and Cu(N3.5) present inductive loops at low frequencies which is associated with film relaxation processes. Table 4 shows the resistance and capacitance values obtained by fitting of the spectra. However, the Cu(N1.5) has a similar spectra profile and resistance values as Cu(N3.5), presenting a charge transfer resistance of 0.52 kΩ cm^2 a capacitance of 111 μF cm^{-2} s^{n-1}, the capacitance reaches the minimum value of 60 μF cm^{-2} at the bulk copper electrode and the maximum value of 259 μF cm^{-2} s^{n-1} is at Cu(N0.0).

These differences in the capacitance and resistance can be attributed first, and mainly, to different structures, roughness as well as grain size of the films, the electrodes with smallest grain

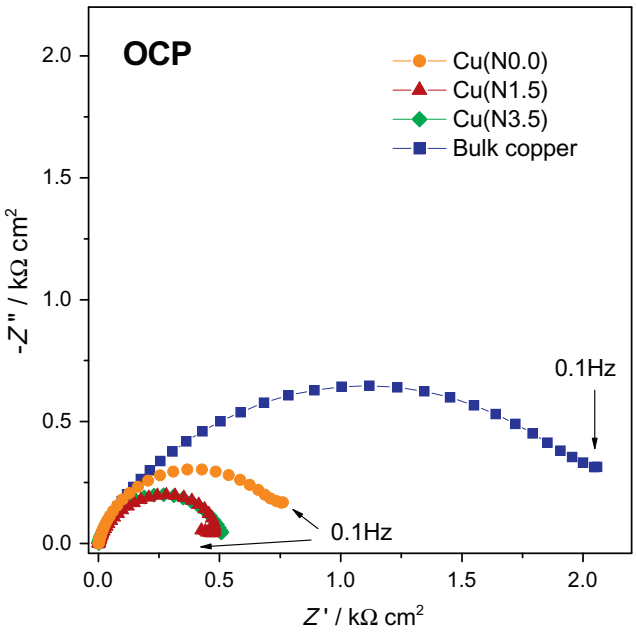

Fig. 4. Complex plane impedance plots in 0.5 M NaCl of: (●) Cu(N0.0), (▲) Cu(N1.5), (◆) Cu(N3.5), (■) bulk copper electrodes at applied potential equal to OCP (see Table 1).

size having the higher surface area. Secondly, the different composition of the film surfaces, with different metal oxides leads to different electrochemical characteristics. Both of these possible contributing factors are confirmed by the SEM characterization discussed below. Additionally, the lower values of the impedance at the more positive potential reflect the effect of enhanced copper dissolution with probable formation of complex species with chloride ion, thus hindering the formation of protective oxide.

The results obtained in the EIS studies are in agreement with those from the polarization curves, and suggest that the Cu(N3.5) film, that exhibits the smallest resistance, has the smallest grain size. This implies that its surface is expected to have a larger number of nanostructures per unit area, resulting in a higher electroactive area.

3.3. Scanning electron microscopy (SEM) characterization of the copper films

Physical and structural characterization of the as-prepared copper films has previously been done by Calinas et al. [2]. In this work the SEM analysis was carried out in order to determine the surface characteristics of the films after corrosion had occurred.

Fig. 5a shows scanning electron micrographs recorded at the Cu(N0.0) electrode, in which the upper surface and that in contact with the steel substrate of a partially peeled film are shown. The white and smooth surface (which contacted the substrate) is free from any corrosion, whereas the other exposed face has undergone corrosion. The latter shows cube-shaped grains of 700 nm diameter over the entire surface, demonstrating that preferential corrosion occurred at the grain boundaries, in this way evidencing the grain nanostructure. The grains are easily seen in Fig. 5b, which shows the same electrode but from a different angle where it is possible to see better the roughness and the "cube-like" aspect of the grains.

The micrographs for Cu(N1.5) and Cu(N3.5) after corrosion, shown in Fig. 6, contrast with those obtained for the film without nitrogen, and the cube-like structures are practically non-existent, being substituted with smaller, irregular structures. It is also seen that in the case of Cu(N1.5), this occurs over the whole electrode

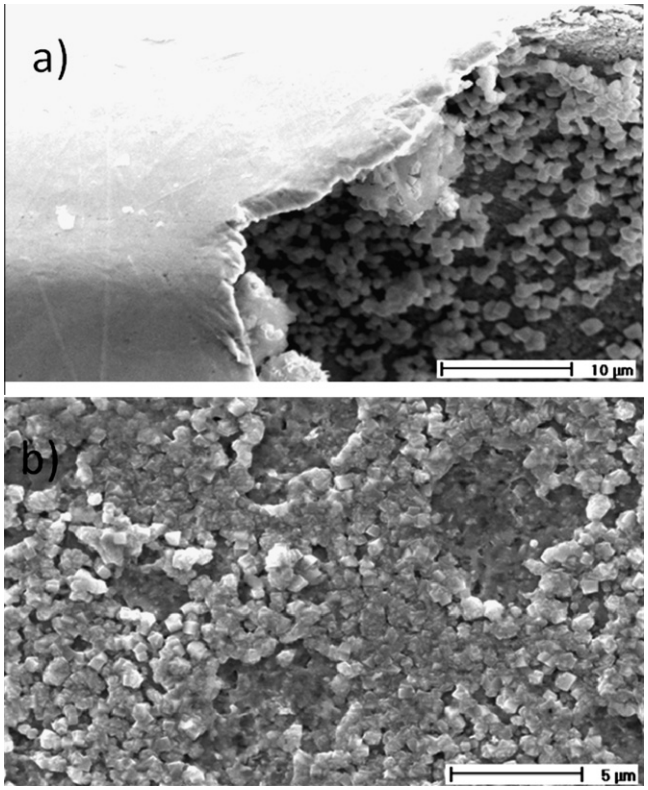

Fig. 5. Scanning electron micrographs of Cu(N0.0) copper thin film (a) folded film (showing surface in contact with substrate) and (b) higher magnification of corroded surface.

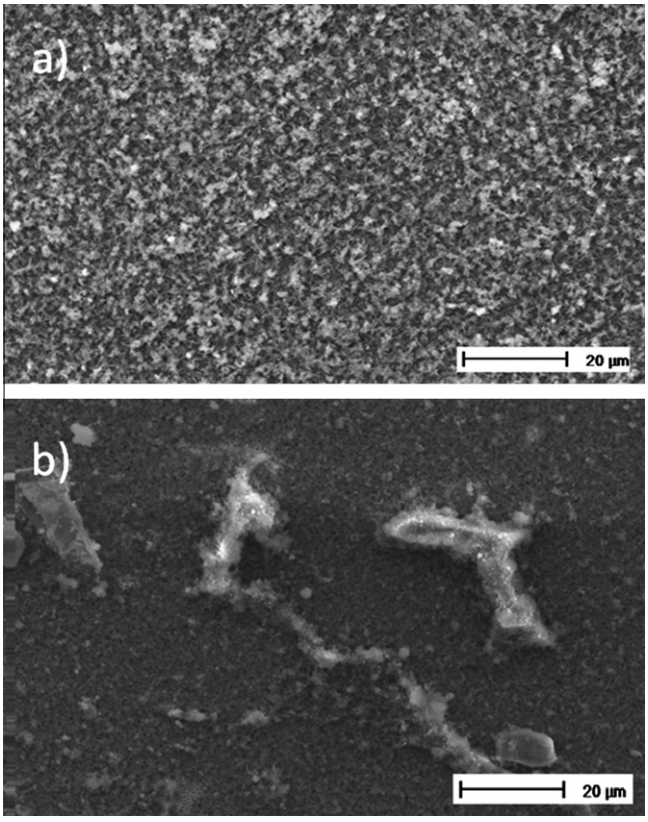

Fig. 6. Scanning electron micrographs of (a) Cu(N1.5) and (b) Cu(N3.5) copper thin films.

surface. However, the most interesting observation was for the Cu(N3.5) film, where there is a mixture of smaller structures together with big deformed structures of more than 30 μm diameter.

Table 2 shows EDX results obtained from electrode surface examination after corrosion, using the same samples. For all electrodes, the presence of chloride and oxygen was detected, from which one can deduce that CuCl and CuO should be formed. This information can be confirmed from the results of atomic percentages of oxygen of 63% and 65% and Cl of 12% and 11% for the electrodes Cu(N0.0) and Cu(N1.5), respectively. For these electrodes, the Cu percentages obtained were 25% and 24%, respectively. Nevertheless, for Cu(N3.5) a high percentage of Cu of 40% was obtained, which indicates that in this case CuCl formation was somehow inhibited, since 54% of oxygen was found, and only 6% of Cl. Nitrogen was not detected although the possible presence of residual nitrogen in the thin films can be deduced from the aspect of some of the thin films during SEM analysis or of thin foils by transmission electron microscopy (TEM). Some of the micro- and nanobubbles in the thin films could be attributed to the desorption of nitrogen during the analyses.

The formation of CuCl grains and their different structure and size can explain the different conductance of the film, and the value of I_{cor} measured for Cu(N3.5). Although this corrosion current was higher than the others, the CuCl and CuO formation was less, from which one can deduce that the dimension of the copper grain interferes with the process of copper oxidation and formation of CuCl.

Films with smaller copper grain size dimensions, Cu(N3.5), have higher corrosion currents, probably due to an increase in the number of grains per unit area leading to an increase in the electroactive surface.

4. Conclusions

This work has shown the influence of the nanocrystalline character of copper thin films on their electrochemical and corrosion behaviour, reflecting the fact that the presence of nitrogen in the sputtering chamber produces copper films with good mechanical and electrochemical properties, due to minimization of grain size and structural defects on the grain frontiers. The corrosion process that occurs on thin films with different surface morphology and grain size may contribute to the formation of different oxide and chloride films. Thin films with smaller copper grain size dimensions have a higher corrosion rate (corrosion current), probably due to an increase in the number of grains per unit area and thus an increase in the electroactive surface area. The EIS studies show convincingly that the electrode with the smallest grain size has lower resistance than the others.

The trends observed by both electrochemical techniques are the same. High reproducibility between the experiments demonstrates that the procedure used for film deposition is highly reproducible, the films having very similar micro/nano-structure, with minimum failures in the nanograin boundaries, which is important for electronic device application.

Acknowledgments

Financial support from Fundação para a Ciência e a Tecnologia (FCT), PTDC/QUI/65255/2006, POCI 2010 and, project POCI/CTM/55970/2004 (co-financed by the European Community Fund FEDER) and CEMUC® (Research Unit 285), Portugal, is gratefully acknowledged. FCT is thanked for EMP's PhD grant (SFRH/BD/31483/2006).

References

[1] P.M. Gordo, M. Duarte Naia, A.S. Ramos, M.T. Vieira, Zs. Kajcsos, Positron studies on nanocrystalline copper thin films doped with nitrogen", in: ICPA15 – 15th International Conference on Positron Annihilation, Kolkata, India), 2009.
[2] R. Calinas, M.T. Vieira, P.J. Ferreira, J. Nanosci. Nanotechnol. 9 (2009) 3921–3926.
[3] J.-M. Welter, Proceedings of the International Conference Copper'06, Wiley-VCH (2006).
[4] R.F. North, M.J. Pryor, Corros. Sci. 10 (1970) 297–311.
[5] R.G. Blundy, M.J. Pryor, Corros. Sci. 12 (1972) 65–75.
[6] R. Vera, G. Layana, J.I. Gardiazabal, Bol. Soc. Chil. Quím. 40 (1995) 149–156.
[7] B. Rosales, R. Vera, G. Moriena, Corros. Sci. 41 (1999) 625–651.
[8] A. Cantor, J. Bushman, M. Glodoski, E. Kiefer, R. Bersch, H. Wallenkamp, Mater. Perfor. 45 (2006) 38–41.
[9] B.J. Miller, J. Electrochem. Soc. 116 (1969) 1675–1680.
[10] V. Ashworth, D. Fairhurst, J. Electrochem. Soc. 124 (1977) 506–517.
[11] K.D. Efird, Corrosion 33 (1977) 3–8.
[12] F. Mansfeld, M.W. Kendig, S. Tsai, Corros. Sci. 22 (1982) 455–471.
[13] D.D. MacDonald, Corrosion 46 (1990) 229–242.
[14] E.M. Sherif, S.-M. Park, J. Electrochem. Soc. 152 (10) (2005) B428–B433.
[15] R. De Marco, R. Eriksen, A. Zirino, Anal. Chem. 70 (1998) 4683–4689.
[16] A. Nagiub, F. Mansfeld, Corros. Sci. 43 (2001) 2147–2171.
[17] A.M. Nagiub, Electrochim. Acta 23 (2005) 301–314.
[18] A. Srivastava, R. Balasubramaniam, Mater. Corros. 56 (2005) 611–618.
[19] S. Jin, S. Amira, E. Ghali, Adv. Eng. Mater 1–2 (2007) 75–83.
[20] D. Silverman, Proceedings of NACE International 1998, Corrosion/98, Houston, TX, Paper 299.
[21] J.A. Beavers, C.L. Durr, N.G. Thompson, Proceedings of NACE International 1998, Corrosion/98, Houston, TX, Paper 300.